



Extraction of actuator forces and displacements involved in human walking and running and estimation of time-series neural signals by inverse dynamics simulation

Motokuni Ishibashi¹ · Kenji Takeda¹ · Kentaro Yamazaki² · Takumi Ishihama¹ · Tatsumi Goto² · Shuxin Lyu¹ · Minami Kaneko² · Fumio Uchikoba²

Received: 23 March 2023 / Accepted: 19 November 2023 / Published online: 5 January 2024
© International Society of Artificial Life and Robotics (ISAROB) 2024

Abstract

While conventional biped robots are arithmetically controlled by CPU and driven by servo motors, humans locomote by contraction of muscles that receive electrical signals from the spinal cord. For real-time control without numerical calculations, we proposed a method that analog electronic circuits mimic neural circuits and output electrical signals. Gait control of a musculoskeletal robot requires this circuit and muscle-mimicking actuators. In this paper, we extracted the muscle displacements and generated forces involved in human walking and running with inverse dynamic simulation. The generated force and electromyogram were compared, and the main moving muscles were selected. The neural signals input to the muscles were derived by dividing the displacement graph into 6 sections and classifying the muscle groups by focusing on the maximum contraction. Also, we compared the generated forces, displacements, and the neural signals with physiological findings and discussed the similarity between the living body and the musculoskeletal model.

Keywords Inverse dynamic simulation · Human musculoskeletal model · Bipedal gait · Muscle · Neural signal

1 Introduction

Because of their similarity to humans, biped robots are expected to play an active role as a substitute for humans and collaborate with humans in various fields. Conventional

biped robots are controlled by a combination of CPU and software programs and driven by servo motors. At this time, the CPU performs computational processing for complex control, including the degrees of freedom of the joints and information from various sensors. As a result, the development is far removed from the structure and function of a living body.

On the other hand, human locomotion is controlled by the spinal cord, and signal patterns for locomotion are generated by the spinal cord [1]. The generated signal patterns are

This work was presented in part at the joint symposium of the 28th International Symposium on Artificial Life and Robotics, the 8th International Symposium on BioComplexity, and the 6th International Symposium on Swarm Behavior and Bio-Inspired Robotics (Beppu, Oita and Online, January 25–27, 2023).

✉ Fumio Uchikoba
uchikoba.fumio@nihon-u.ac.jp

Motokuni Ishibashi
csmo21005@g.nihon-u.ac.jp

Kenji Takeda
cskn20001@g.nihon-u.ac.jp

Kentaro Yamazaki
cstt19053@g.nihon-u.ac.jp

Takumi Ishihama
csjo21031@g.nihon-u.ac.jp

Tatsumi Goto
cske19138@g.nihon-u.ac.jp

Shuxin Lyu
cstk22005@g.nihon-u.ac.jp

Minami Kaneko
takatou.minami@nihon-u.ac.jp

¹ Graduate School of Science and Technology, Nihon University, Chiba, Japan

² College of Science and Technology, Nihon University, Chiba, Japan

transmitted to muscles as nerve pulses via motor neurons, causing muscle contraction and movement [2]. Despite the simplicity of the mechanism, advanced, flexible, and real-time control and locomotion are achieved.

An example of research on robots that mimic the human skeleton and muscles without the conventional biped robot mechanism is a musculoskeletal full-body robot in which pneumatic artificial muscles are driven by control signals from a microcontroller [3]. Pneumatic artificial muscles are used as actuators, enabling dynamic movement with high output. A control system for artificial muscles that mimics the neural circuits of a living body with a microcontroller has also been developed [4]. This system is controlled by software-based arithmetic processing.

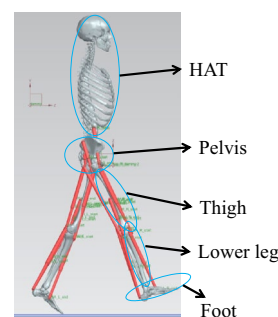
On the other hand, we proposed a numerically non-computational control method that uses analog electronic circuits to mimic neural circuits and output electrical signals [5]. In this previous paper, we divided one cycle into six and created the presence or absence of the second and third pulses to simulate the neural signals of walking and running. This means that the developed neural network has been able to reproduce the physiological finding from electromyography measurements that there is a difference between walking and running with 5 pulses per cycle, and the timing of the second pulse appearing earlier or later [6].

Although it lacks flexibility, because the parameters are incorporated as circuit constants, it handles electrical signals directly and thus enables real-time control that does not depend on calculations. Compared to software control, this control is very close to signal transmission in the human nervous system. The use of MOSFETs is also expected to make it possible to create ICs. To control the walking motion of a musculoskeletal robot with this analog electronic circuit, a linear actuator that mimics human muscles is required.

However, the proposed artificial neural network provides only timing for each muscle actuator to walking and running. The displacement and force required for the walking motion are unclear, and it is not clear at what timing the parameters should be input.

Therefore, this paper uses inverse dynamics simulation to extract the muscle displacements and generated forces involved in human walking and running as actuator parameters. From the extracted parameters, neural signals were derived. The extracted parameters and the derived neural signals were then compared with actual physiological findings and discussed.

Fig. 1 Human musculoskeletal model



2 Structures of the human musculoskeletal model

2.1 Skeleton and scale

The human musculoskeletal model consists of a skeleton and muscles and is designed based on the 3D anatomy man [7]. Figure 1 shows the model. The skeleton consists of five parts: HAT (Head, Arm, Trunk), pelvis, thigh, lower leg, and foot. Table 1 shows the length and weight of the skeleton. The scale of the skeleton was set to one-half the life-size of a human model for the sake of easy fabrication and verification of the robot in the future. We also measured weight of those skeletons that we made with 3D printer by Table 1 scale.

The joints of this model are also described. There are four joints that perform rotational motion: the sacroiliac joint, hip joint, knee joint, and ankle joint. The human walking motion is a three-dimensional motion that includes flexion, extension, and rotation. In this study, it was assumed that the turning motion is slight and has no significant effect on the walking motion. Therefore, the four joints were constrained to operate only in a two-dimensional plane, and each leg was analyzed. With respect to the sacroiliac joints, making the degrees of freedom two-dimensional also served to constrain the entire model to the sagittal plane.

2.2 Muscle selection and movement

Human locomotion is generated by a complex interplay of skeletal, muscular, and nervous systems and is extremely complex. Therefore, it is very difficult to reproduce all of them as a musculoskeletal model. However, if we focus on walking movements and use the effective muscle concept, we can reproduce leg movements with some of the major muscles [6, 8]. Musculoskeletal model muscles are redundant systems, so estimating internal muscle strength is complicated. In this paper, we focused on the muscles that generate large amounts of muscle strength related to

Table 1 Length and weight of skeletal

Skeleton	HAT (Head, Arms, Trunk)	Pelvis	Thigh	Lower leg	Foot	Total
Length [mm]	284	100	220	164	36	804
Weight [g]	201.1	37.3	48.6	34.2	17.1	338.3

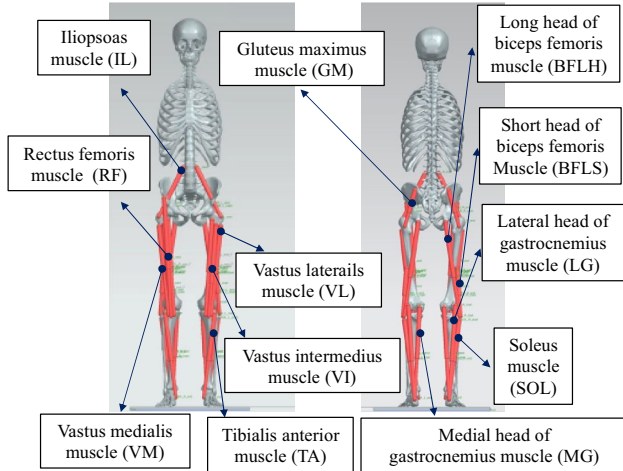


Fig. 2 Muscle composition

walking. There are nine effective muscles, six monoarticular and three biarticular, which work to rotate one joint, whereas biarticular muscles work across two joints and rotate different joints or both joints, depending on the movement. The six monoarticular muscles have three pairs of antagonist muscles, and for the three biarticular muscles, there is one antagonist muscle pair.

In this model, the 9 effective muscles were subdivided into 12 different muscles. Figure 2 shows the composition of the muscles [9]. The muscles were: Iliopsoas lumborum (IL), Gluteus maximus (GM), Rectus femoris (RF), Vastus intermedius (VI), Vastus lateralis (VL), Vastus medialis (VM), Long head of biceps femoris (BFLH), Short head of biceps femoris (BFSH), Tibialis anterior (TBA), Lateral gastrocnemius head (LG), Medial gastrocnemius head (MG), and Soleus muscle (SOL). Some of the effective muscles are represented as a grouping of several muscles, and these include the vastus adductus (VA) and gastrocnemius (GC). We considered that subdividing these two muscles would allow us to extract more lifelike muscle parameters, so we selected 12 muscles for the human musculoskeletal model. In 12 muscles, IL, GM, VI, VL, VM, BFSH, TBA, and SOL are divided into 1-joint muscles; and RF, BFLH, LG, and MG are divided into 2-joint muscles.

The muscles are also designed based on the 3Danatomyman. Muscles are typically modeled as actuators that

Table 2 Length and weight of muscles

Muscle	Length[mm]	Weight[g]
Iliopsoas muscle (IL)	182.10	7.00
Gluteus maximus muscle (GM)	131.70	4.80
Rectus femoris muscle (RF)	261.14	14.04
Vastus intermedius muscle (VI)	197.13	11.61
Vastus lateralis muscle (VL)	221.41	10.72
Vastus medialis muscle (VM)	195.68	10.08
Long head of biceps femoris muscle (BFL)	207.47	11.36
Short head of biceps femoris muscle (BFS)	145.72	5.87
Tibialis anterior muscle (TA)	174.85	9.83
Lateral head of gastrocnemius muscle (LG)	130.59	11.36
Medial head of gastrocnemius muscle (MG)	145.28	10.72
Soleus muscle (SOL)	134.21	9.19

include viscosity and elasticity. However, in this paper, we first assume a simple cylinder linear actuator, and then find the actual actuator requirements from the obtained parameters. The length of the 12 muscles is one-half the scale of the human body, and the weight is calculated by Eq. (1). Lengths and weights of the 12 muscles are shown in Table 2 [10]. The locations of muscle attachments in Fig. 2 are based on anatomical origin and stop locations

$$\text{Skeleton length} : \text{Muscle length} = \text{Skeleton weight} : \text{Muscle weight.} \tag{1}$$

3 Walking and running in a human musculoskeletal model

The human musculoskeletal model described in Chapter 2 was used to analyze the dynamics of walking and running and to extract parameters for the linear actuator. Since this study focuses on walking and running motions, the model was fixed on the sagittal plane. Simcenter 3D from SIEMENS was used for the dynamics analysis.

As a parameter extraction method, the joint angles of human walking and running were first input to the hip, knee, ankle, and sacroiliac joints of the human

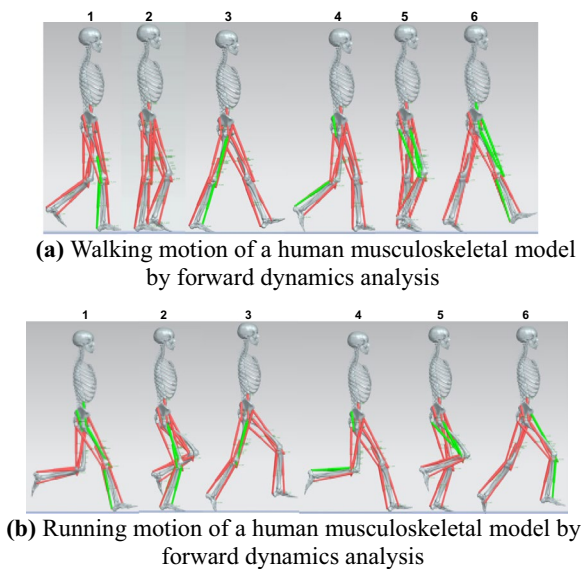


Fig. 3 Forward dynamic analysis of a human musculoskeletal model

musculoskeletal model, and the amount of displacement of each muscle was calculated by forward dynamic analysis. Each joint angle for walking and running was obtained from data published in open-source software used in biomechanics research [11]. For each joint angle, displacements for one gait cycle were used. In gait analysis, one gait cycle is defined as two steps per leg. In this model, the right leg was used as the reference leg and two steps were used as one gait cycle. Next, the displacement calculated by the forward dynamics analysis was input to the linear actuator, and the force generated by each muscle was calculated by the inverse dynamics analysis. The walking cycle was set to 0.96 s for both cases. Figure 3 shows the walking and running motions of the human musculoskeletal model based on forward dynamics analysis.

4 Muscle displacement, force, and nerve signals

Figure 4 shows the force generated by each muscle during walking extracted by inverse dynamics analysis. Figure 5 shows the force generated by each muscle during running extracted by inverse dynamics analysis. The generated forces of the extracted muscle time-series were matched with electromyograms taken from the literature [6, 12]. Ten types of lower limb electromyogram (EMG) potentials contributing to walking and running were used. The muscles used in the musculoskeletal model were 12 muscles per side, but in mapping them, the short head of the biceps femoris and the

vastus medialis of the deep muscles, which are difficult to obtain EMG potentials, were excluded.

The displacement and force generated obtained from the musculoskeletal model also include when the muscle is being stretched. However, since the muscle exerts force only during contraction, it is necessary to focus on the direction of contraction. In the direction of contraction, the generated force and timing of muscle activity were very close in eight muscles (BFLH, IL, LG, MG, SOL, TBA, VL, and VM) in walking compared to muscle potentials. In running, the generated force and timing of muscle activity were very close in seven muscles (BFLH, GM, LG, MG, SOL, VL, and VM). Therefore, these muscles were presumed to be the muscles that mainly contracted during walking and running.

Specifically, muscle movement, displacement, and generated force are compared. Table 3 shows the maximum displacement and the maximum generated force during walking, and Table 4 shows the maximum displacement and the maximum generated force during running.

Horizontal column 1~6 in Table 3 and 4 represents time regions in which one cycle of walking motion is divided into 6 segments. This is based on the neural network we developed previously, which divides one cycle into six and controls walking and running based on the presence or absence of pulses in the second and third regions. Physiological findings from electromyography measurements are analyzed using 5 pulses per cycle, and it has been reported that the difference between walking and running is whether the second pulse appears earlier or later. If a pulse appears in the second region and does not appear in the third region in a region temporally divided into 6 regions, it means that the second pulse appears earlier. If a pulse appears in the third region and does not appear in the second region, it means that the second pulse appears late.

In walking, the knee joint is flexed from the third to the fourth timing in Fig. 3a. In this case, for example, the MG shows the largest muscle potential at the third timing. And contraction started at the same time, followed by the largest contraction in the MG movement. As for the generated force, it occurred at the same timing as the muscle potential, and the maximum generated force was output at the fourth timing. The parameters were 4.22 N of generated force and 1.01 mm of displacement at the third timing, and 7.65 N of generated force and 18.42 mm of displacement at the fourth timing, confirming the consistency with the motion and graph. Therefore, the parameters extracted for walking were considered valid. In running, hip flexion takes place from the third to the fifth timing in Fig. 3b, and the thigh is sent forward. At this time, for example, the largest muscle potential is observed at the first timing in the LG. And it was confirmed that contraction started at the same time. The maximum force generated was output at the second timing.

Fig. 4 Force of each 12 muscles during walking

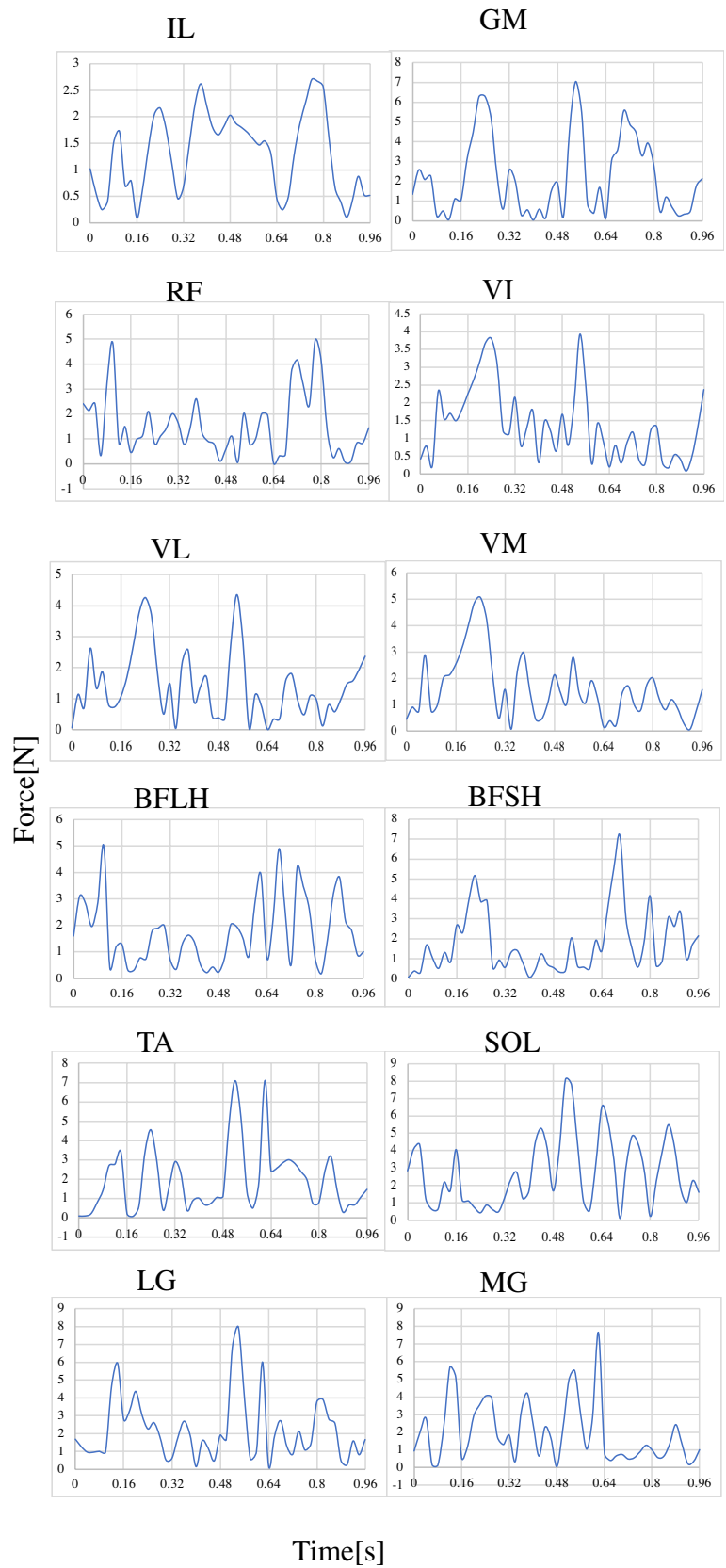


Fig. 5 Force of each 12 muscles during running

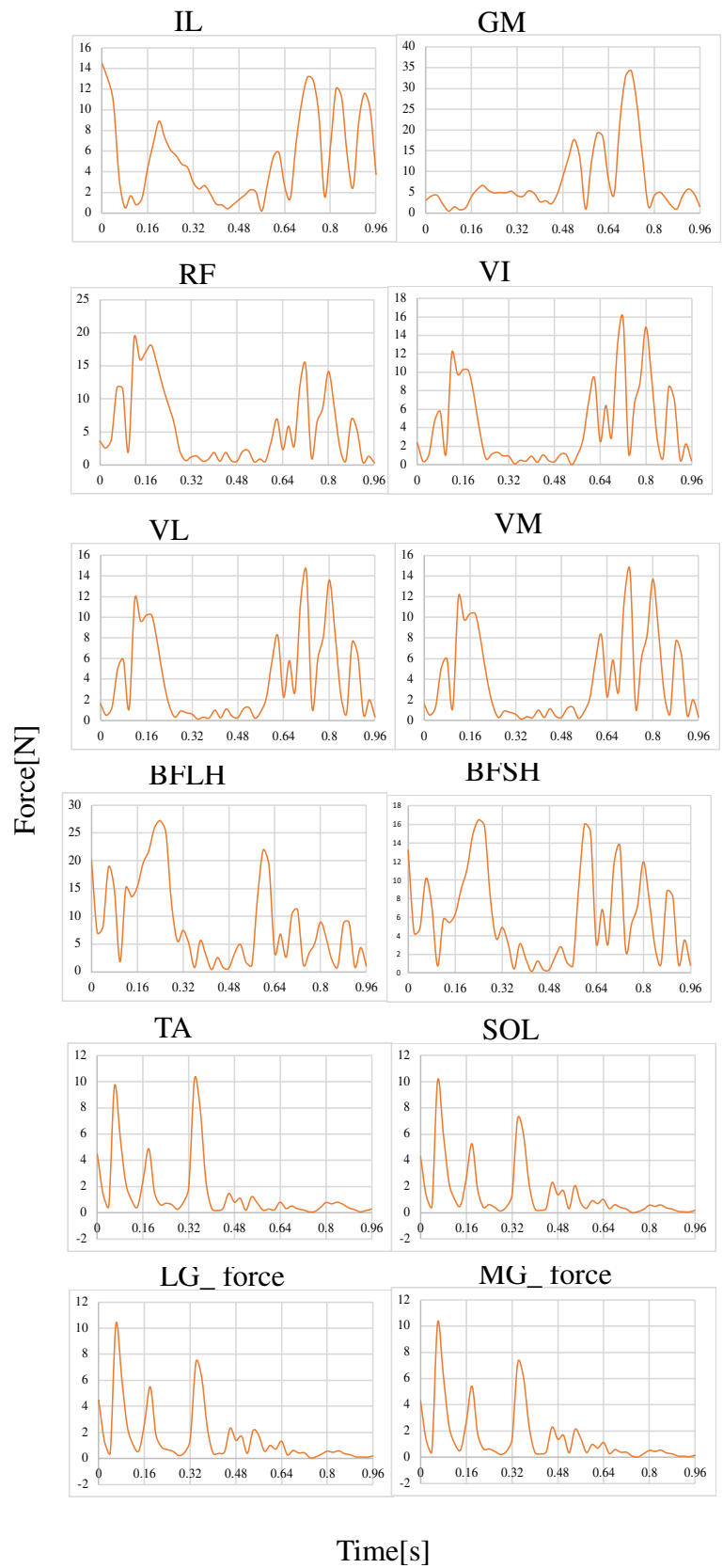


Table 3 Amount of muscle contraction and force generated during walking

	1		2		3		4		5		6	
	Displacement [mm]	Force [N]	Displacement [mm]	Force [N]	Displacement [mm]	Force [N]	Displacement [mm]	Force [N]	Displacement [mm]	Force [N]	Displacement [mm]	Force [N]
IL	0.00	1.72	0.00	2.16	0.00	2.62	0.92	1.88	3.38	2.70	0.63	1.57
GM	2.20	2.58	6.12	6.29	5.66	2.01	0.40	7.03	0.00	5.56	0.11	1.76
RF	0.00	4.84	0.00	2.11	0.00	2.62	1.29	2.00	9.75	4.97	11.21	1.37
VI	0.04	2.32	2.21	3.80	0.88	1.78	0.26	3.92	1.57	1.17	4.60	1.34
VL	0.17	2.62	2.21	4.26	0.64	2.58	0.21	4.35	1.17	1.80	4.93	1.95
VM	0.13	2.90	2.23	5.07	0.76	2.99	0.21	2.80	1.28	1.71	4.94	1.23
BFLH	8.27	5.00	6.37	1.99	6.51	1.64	9.01	3.93	0.34	4.90	0.00	3.83
BFSH	1.68	1.69	0.00	5.17	0.38	1.41	8.16	1.92	3.70	7.17	0.00	3.35
TBA	2.93	3.41	2.43	4.55	1.66	2.28	0.00	7.08	5.75	3.00	0.40	3.17
SOL	1.44	4.34	0.00	1.15	0.15	5.28	10.33	8.07	0.00	5.66	0.90	5.48
LG	4.04	5.95	0.00	4.37	0.58	2.70	20.46	7.97	0.13	2.72	0.00	3.93
MG	3.80	5.68	0.00	4.06	1.01	4.22	18.42	7.65	0.00	1.26	0.00	2.43

Table 4 Amount of muscle contraction and force generated during running

	1		2		3		4		5		6	
	Displacement [mm]	Force [N]	Displacement [mm]	Force [N]	Displacement [mm]	Force [N]	Displacement [mm]	Force [N]	Displacement [mm]	Force [N]	Displacement [mm]	Force [N]
IL	0.00	10.77	0.84	8.90	0.00	2.65	1.26	5.39	5.79	13.16	2.05	8.76
GM	2.33	4.21	1.95	6.63	10.43	5.29	0.54	19.20	0.00	34.22	0.00	0.55
RF	0.00	11.66	0.00	18.10	0.00	1.85	5.76	6.96	28.41	15.18	2.87	8.76
VI	2.21	5.72	0.28	10.15	1.67	1.09	5.78	9.40	14.46	15.88	0.00	8.38
VL	2.27	5.84	0.16	10.14	1.84	1.11	4.93	8.20	13.06	14.41	0.00	7.55
VM	2.31	11.99	0.16	10.31	1.80	1.13	4.99	8.30	13.19	14.55	0.00	7.63
BFLH	3.65	18.87	15.93	27.18	7.40	5.61	20.91	21.95	3.54	11.11	0.00	11.19
BFSH	0.33	10.17	6.85	16.50	0.12	3.21	16.64	16.02	13.83	13.64	0.00	0.57
TBA	0.00	9.65	10.10	4.89	0.00	10.17	2.60	1.22	8.03	0.51	1.89	0.80
SOL	2.03	6.08	1.04	5.27	18.38	7.19	1.46	2.08	0.00	0.62	0.02	0.60
LG	0.97	10.31	3.24	5.49	12.90	7.38	9.04	2.12	0.00	0.60	0.18	0.60
MG	0.91	10.23	2.88	5.42	13.81	7.25	5.96	2.12	0.00	0.58	2.18	0.80

Fig. 6 Displacement of each 12 muscles during walking

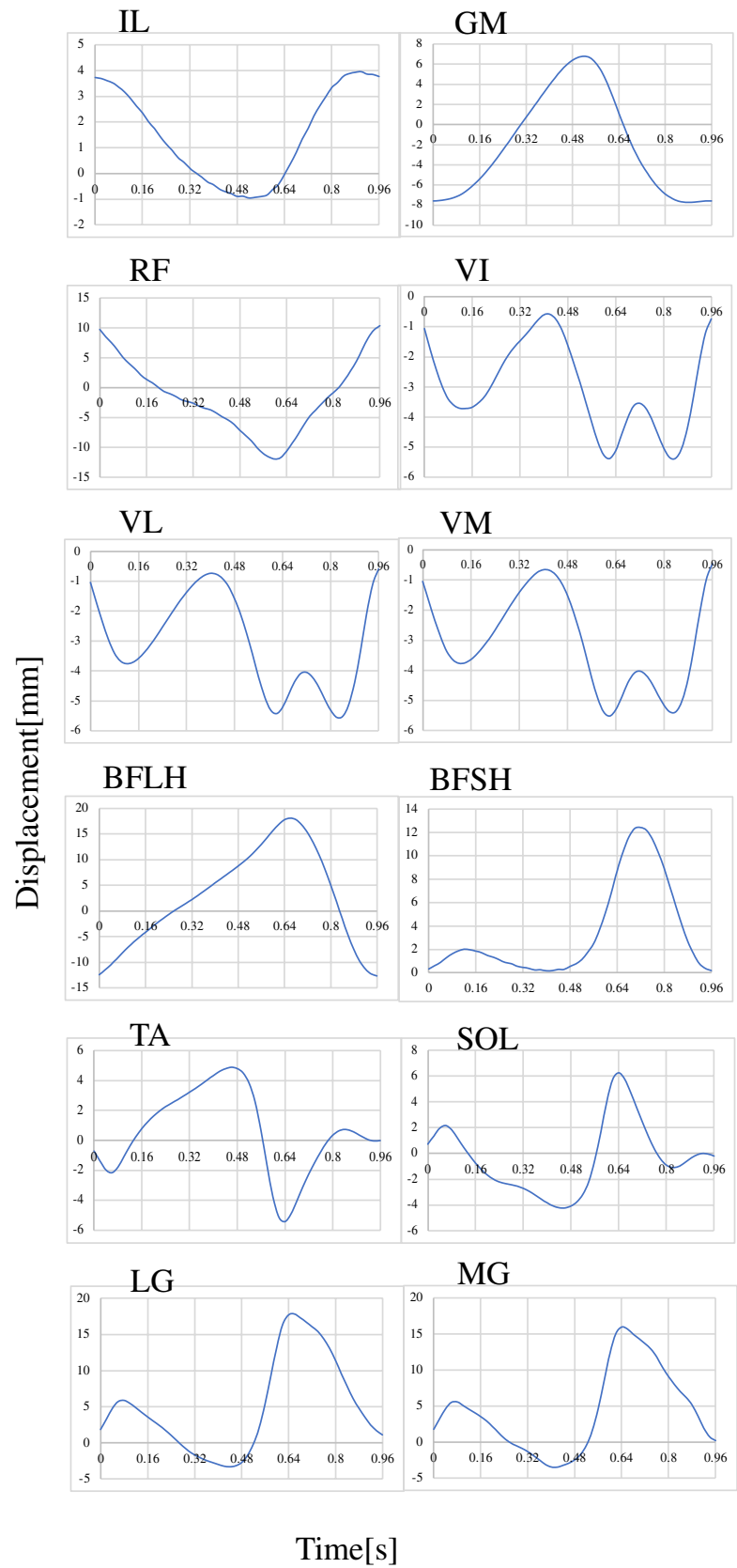


Fig. 7 Displacement of each 12 muscles during running

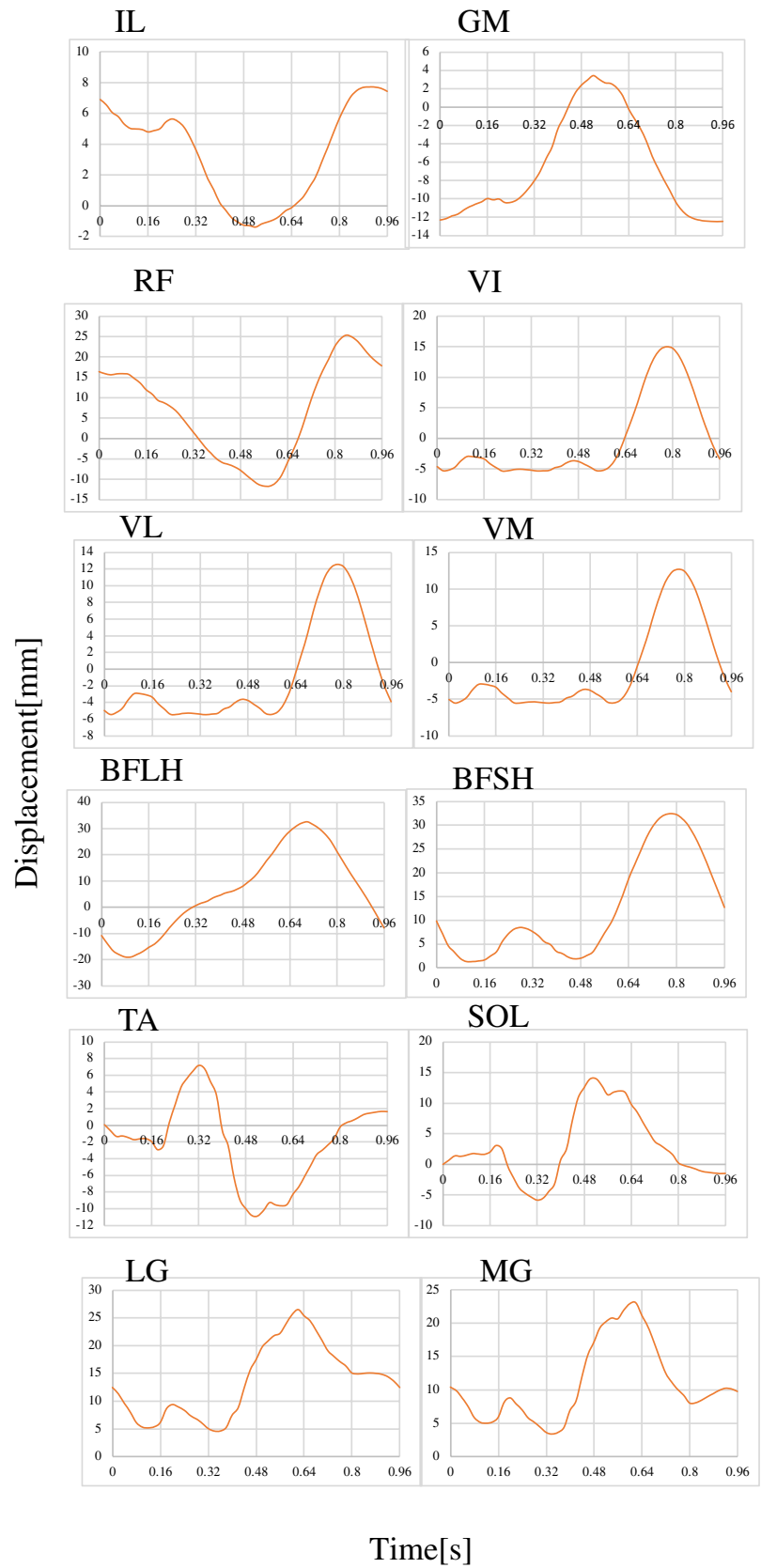


Table 5 Classification of walking muscles

Muscle	1	2	3	4	5	6
IL						○
GM				○		
RF						○
VI			○		○	○
VL			○		○	○
VM			○		○	○
BFLH					○	
BFSH	○				○	
TA			○			○
SOL	○			○		○
LG	○				○	
MG	○			○		

Table 6 Classification of running muscles

Muscle	1	2	3	4	5	6
IL		○				○
GM	○			○		
RF						○
VI	○	○	○		○	
VL	○	○	○		○	
VM	○	○	○		○	
BFLH					○	
BFSH		○			○	
TA		○		○		○
SOL		○		○		
LG		○		○		
MG		○		○		○

Table 7 Classification of muscles during walking in correspondence with EMG

Muscle	1	2	3	4	5	6
IL						○
VL			○		○	○
VM			○		○	○
BFLH					○	
SOL	○			○		○
TA			○			○
LG	○				○	
MG	○			○		

Although the force generated at the first timing was greater than the force generated at the second timing, the graph shows that the force generated at the first timing was not the force being exerted for contraction. The force generated by the first is thought to be exerted to hold the torso in place when the foot is stepped on the ground.

Focusing on the displacements of walking and running, the neural signals were estimated by targeting the maximal contractile displacement of each muscle. Figure 6 shows the displacement of each muscle during walking extracted by forward dynamics analysis Fig. 7 shows the displacement of each muscle during running extracted by forward dynamics analysis. The graph of displacement for each muscle was divided into 6 sections and plotted where the contraction was maximal.

The classified muscle groups are shown in Table 5, 6, 7, 8. In addition, the muscles shown in green in Fig. 3 reflect Table 5, 6, 7, 8. Table 5 classifies the muscles that are displaced in the direction of contraction during walking by timings 1~6. The corresponding muscles are circled. Table 6 classifies the muscles that are displaced in the direction of contraction at the time of running by timings 1~6. The corresponding muscle is marked with a circle, similarly. Table 7 shows the muscles that were placed during gait and agreed with the position of action potentials and contractile force generation by comparing EMG and force at timings 1–6. These muscles were defined as the main active muscles involved in the walking movement. Muscles that were displaced in the direction of contraction were marked with a circle. Table 8 shows the muscles that were placed during running, and the muscles that showed agreement in the position of action potentials and contractile force generation were extracted at timings 1–6 by comparing EMG and force similarly. These muscles were defined as the main active muscles involved in the walking movement. Muscles that were displaced in the direction of contraction were marked with a circle. The blue markings in Tables 5, 6, 7, 8 represent the timings where there is a marked difference in the number of muscles contracting between walking and running at timings 1~6. In walking, no maxima were observed at the second timing, and not many contractions were observed. In running, the second timing of the maximal point was observed, and contraction was observed in large numbers. The same was true for the eight muscles in walking and seven muscles in running. From these results, it can be said that the humanoid musculoskeletal model operates at timings 1, 3, 4, 5, and 6 in walking, and at timings 1, 2, 4, 5, and 6 in running. In other words, the second timing is the point of distinction between walking and running, we found the signal timing to control walking and running and inferred that when the walking cycle is divided into 6 segments, the neural signal inputs for walking are 1, 3, 4, 5, and 6, and for running, 1, 2, 4, 5, and 6.

Table 8 Classification of muscles during running in correspondence with EMG

Muscle	1	2	3	4	5	6
GM	○			○		
VL	○	○	○		○	
VM	○	○	○		○	
BFLH					○	
SOL		○		○		
LG		○		○		
MG		○		○		○

Focusing on the displacements of walking and running, the neural signals were estimated by targeting the maximal contractile displacement of each muscle. Figure 6 shows the displacement of each muscle during walking extracted by forward dynamics analysis. Figure 7 shows the displacement of each muscle during running extracted by forward dynamic analysis. The graph of displacement for each muscle was divided into 6 sections and plotted where the contraction was maximal. The classified muscle groups are shown in Table 5, 6, 7, 8. In addition, the muscles shown in green in Fig. 3 reflect Table 5, 6, 7, 8. Table 5 classifies the muscles that are displaced in the direction of contraction during walking by timings 1~6. The corresponding muscles are circled. Table 6 classifies the muscles that are displaced in the direction of contraction at the time of running by timings 1~6. The corresponding muscle is marked with a circle, similarly. Table 7 shows the muscles that were placed during gait and agreed with the position of action potentials and contractile force generation by comparing EMG and force at timings 1–6. These muscles were defined as the main active muscles involved in the walking movement. Muscles that were displaced in the direction of contraction were marked with a circle. Table 8 shows the muscles that were placed during running, and the muscles that showed agreement in the position of action potentials and contractile force generation were extracted at timings 1–6 by comparing EMG and force similarly. These muscles were defined as the main active muscles involved in the walking movement. Muscles that were displaced in the direction of contraction were marked with a circle. In walking, no maxima were observed at the second timing, and not many contractions were observed. In running, the second timing of the maximal point was observed, and contraction was observed in large numbers. The same was true for the eight muscles in walking and seven muscles in running. From these results, it can be said that the humanoid musculoskeletal model operates at timings 1, 3, 4, 5, and 6 in walking, and at timings 1, 2, 4, 5, and 6 in running. In other words, the second timing is the point

of distinction between walking and running, we found the signal timing to control walking and running and inferred that when the walking cycle is divided into 6 segments, the neural signal inputs for walking are 1, 3, 4, 5, and 6, and for running, 1, 2, 4, 5, and 6.

5 Discussion

The similarities between the human and musculoskeletal models are discussed based on the extracted muscle generating forces and displacements and the estimated neural signals. The timing of EMG activity and the timing of maximum force generation for each muscle used to estimate the primary muscles during walking and running are not perfectly aligned in timing either. There is a slight discrepancy from the time the EMG potential is input until the muscle generates force. This is not considered a problem, because it has been suggested that it takes about 50[ms] for the muscle to generate the target force [13].

In addition, muscles that were not timed are considered to be operating passively. Muscles exert force only when they contract, but not necessarily when they are contracted. One such example could be trunk retention. In other words, the muscles that were not timed can be considered to have been exerting force because of trunk retention. In addition, since the muscles are reproduced with a single cylinder in this model, they are highly dependent on contraction. This effect may have delayed the timing. Originally, muscles are attached to the skeleton at two end points, the starting point and the stopping point. When nerve pulses are transmitted to the muscle, thin filaments of actin slip between thick filaments of myosin and contract. In terms of muscle action, the sliding in and out of the cylinder can be thought of as the sliding of filaments, so the contraction action is considered to be physiologically consistent. In terms of muscle attachment, however, there is not necessarily a single point of attachment. Therefore, it is thought that more accurate values may be calculated by increasing the number of cylinders according to the number of attachment points for each muscle and calculating the average value of displacement and force of the cylinders.

The neural signals obtained from physiological findings were then compared with those derived in this study. Physiologically, it has been shown that most walking movements can be reconstructed with a combination of five muscle action potentials, classified by correlated waveforms, among the muscle potentials measured during walking movements. It has also been shown that in running, the second of the five waveforms is output earlier than in walking [7]. We divided one cycle of walking motion into six time regions to verify the classification of neural signals during walking motion due to muscle

contraction with physiological findings and to facilitate handling of the second signal, in which the difference between walking and running appears. The central pattern generator (CPG), which is localized in the spinal cord and is believed to control basic and periodic movements, generates five time-series signal patterns and is thought to switch between walking and running by changing the position of the second waveform [7]. In this study, neural signals were derived by dividing the displacements extracted during walking motion in a human musculoskeletal model into six regions. In physiological findings, the difference between walking and running is the location of the second neural signal. In this study, we found that signals were generated at timings 1, 3, 4, 5, and 6 during walking, and at timings 1, 2, 4, 5, and 6 during running. The difference between walking and running is the presence or absence of the second and third signals. In other words, the absence of either the second or the third signal is considered to switch between walking and running. This is consistent with physiological findings that the switching between walking and running depends on whether the second signal is generated earlier or later in time. However, it cannot be said that the neural signals derived in this study completely separate the second and third signals. In particular, contraction was observed at the third timing in Table 6 for running. Since the amount of contraction is small (1.67 ~ 1.84[mm] for all muscles), the effect is considered to be small, but it cannot be said that the third signal is not completely output. This may be due to the fact that it is not completely distinguishable whether the contraction of the muscle being performed was done primarily or passively. Therefore, we believe that a more detailed neural signal can be derived by completely distinguishing between principal and passive contractions, and by performing kinetic analysis by inputting the principal contraction force to the muscle.

6 Conclusion

In this paper, we extracted the displacements and generated forces of the muscles involved in human walking and running using a human musculoskeletal model by inverse dynamics simulation. After dividing one cycle of the force generating into 6 segments, we selected the main active muscles during walking and running by comparing them with the muscle potentials. The timing of nerve signals input to the muscles was estimated by dividing one cycle of the extracted displacement into 6 segments and classifying the muscle groups by focusing on the maximum contraction displacement. The extracted generated forces, displacements, and the estimated neural signals were

compared with physiological findings and discussed the similarity between the living body and the musculoskeletal model.

By extracting muscle contraction displacement and the force generated, we discussed from an engineering perspective what kind of signals should be given to the muscles to enable walking movements that imitate humans. The results showed that, similar to physiological findings, walking motion engineering can be generated by inputting five periodic signal patterns. In our paper, we treated the 5 periodic signal patterns as the variations in the appearance of his 5 pulses in his 6 time division regions.

In this study, we qualitatively compared the muscle contraction displacement and generated force extracted from a musculoskeletal model with physiological knowledge, and discussed the generated force and displacement, which are actuator parameters, in the time domain. We also demonstrated engineering that the input signals to muscles differ at specific times when walking and running. We plan to use these results to build an actual machine and further verify the validity of muscle contraction displacement and generated force.

Acknowledgements This study was supported in part by JSPS KAKENHI, Grant-in-Aid for Scientific Research JP22K04016. Also, this work was partially supported by the research grant of Nihon University and NUROS.

Data availability The datasets generated and/or analyzed during the current study are available from the corresponding author on reasonable request.

References

1. Minassian K, Hofstoetter US, Dzeladini F et al (2017) The human central pattern generator for locomotion: Does it exist and contribute to walking. *Neuroscientist* 23(6):649–663
2. Akazawa K (2001) *Bioinformation engineering*. Tokyo Denki University Press, Tokyo (**In Japanese**)
3. Ogawa K, Narioka K, Hosoda K (2010) Stabilization of standing posture by pneumatic artificial musculoskeletal humanoid robot. *Proc 2016 JSME Conf Robotics Mechatron* 2010(10):2A2-D19(1)-2A2-D19(4) (**In Japanese**)
4. Kawakami T, Shin H, Yamanishi T et al (2016) Development of PAM control system inspired by biological neural circuit. *Proc JSME Conf Robotic Mechatron*. 2016(16–2):2P2-11b5(1)-2P2-11b5(3) (**In Japanese**)
5. Takeda K, Ishibashi M, Ishihama T, Aibara M, Kaneko M, Uchikoba F (2022) The walking and running control of a human musculoskeletal model using a low-power consumption hardware central pattern generator model. *Int J Adv Robotic Syst*. <https://doi.org/10.1177/17298806221080633>
6. Ivanenko YP, Poppele RE, Lacquaniti F (2004) Five basic muscle activation patterns account for muscle activity during human locomotion. *J Physiol* 556(1):267–282
7. 3DAnatomyman- Free Male Anatomy 3Dmodel, <https://always3d.gumroad.com/l/haJWL>. Accessed 5 December 2022

8. Aoi S, Ohashi T, Bamba R et al (2019) Neuromusculoskeletal model that walks and runs across a speed range with a few motor control parameter changes based on the muscle synergy hypothesis. *Sci Rep* 9(369):1–13
9. Winter DA (2019) *Biomechanics and motor control of human movement*. John Wiley & Sons Inc, Hoboken
10. Ishii N, Ymaguchi N, Sa M (2012) *The Basics of Muscles and Their Mechanisms by Movement*, MyNavi Corporation Tokyo.
11. OpenSim, <https://simtk.org/projects/opensim>. Accessed 3 October 2022
12. Cappellini G, Ivanenko YP, Poppele RE et al (2006) Motor patterns in human walking and running. *J Neurophysiol* 95(6):3426–3437
13. Fukunaga T (2002) *Encyclopedia of muscle science: structure, function and motion*. Asakura Publishing Tokyo, Tokyo (**In Japanese**)

Publisher's Note Springer Nature remains neutral with regard to jurisdictional claims in published maps and institutional affiliations.

Springer Nature or its licensor (e.g. a society or other partner) holds exclusive rights to this article under a publishing agreement with the author(s) or other rightsholder(s); author self-archiving of the accepted manuscript version of this article is solely governed by the terms of such publishing agreement and applicable law.